Fuel Processing Technology 121 (2014) 83–90

Contents lists available at ScienceDirect

Fuel Processing Technology

journal homepage: www.elsevier.com/locate/fuproc

Experiments and analysis of propagation front under gasification regimes in a packed bed

Sadhan Mahapatra, S. Dasappa *

Centre for Sustainable Technologies, Indian Institute of Science, Bangalore 560 012, India

ARTICLE INFO

Article history:
Received 4 July 2013
Received in revised form 8 January 2014
Accepted 11 January 2014
Available online 1 February 2014

Keywords:
Flame front
Propagation rate
Packed bed
Biomass gasification

ABSTRACT

The paper analyses the results of experiments on the propagation rate in a fuel bed under gasification conditions in a co-current reactor configuration. Experiments using wood chips with different values of moisture content have been conducted under gasification conditions. The influence of air mass flux on the propagation rate, peak temperature and gas quality is investigated. It is observed from the experiments that the flame front propagation rate initially increases as the air mass flux increased, reaching a peak propagation rate, and further increase in the air mass flux results in a decrease in the propagation rate. However, the bed movement increases with the increase in air mass flux. The experimental results provide an understanding on influence of the fuel properties on propagation front. The surface area per unit volume of the particles in the packed bed plays an important role in the propagation rate. It has been argued that the flaming pyrolysis contributes towards the flame propagation as opposed to the overall combustion process in a packed bed. The calorific value of the producer gas generated is nearly the same over the entire range of air mass flux for bone-dry and 10% moist wood.

1. Introduction

Gasification, a sub-stoichiometric combustion process, converts solid fuel to gaseous fuel. During this process, the fuel undergoes thermochemical processes like drying, pyrolysis, and heterogeneous and homogenous combustion. Unlike in combustion, where the primary intention is to release all the energy as sensible heat, in the case of gasification, the energy is transferred to combustible gaseous species. The entire process occurs under fuel rich conditions. Each of these processes has a specific time scale depending upon the properties of biomass like density, thermal conductivity, particle size, and moisture, and also the reactive environment surrounding the particle. The propagation front in a packed bed can be classified as forward and reverse propagation depending upon the relative direction of the air and fuel movement. In reverse propagation, the flame front propagates in a direction opposite to that of air mass flux. In the case of forward propagation, the propagation flame front moves in the same direction as oxidizer flow. The rate of the propagating front movement is primarily controlled by air mass flux, volatile fraction of the fuel and the surrounding reaction environment of the particle.

In the case of a packed bed, depending upon the air flow rate, propagation flame front moves into the virgin fuel. The propagation rate, which is influenced by air flow, combustion and heat transfer, depends on the fuel properties like size, density, thermal conductivity, moisture content, ash content and calorific value. However, not all these parameters are independent variables. Most of the above listed parameters are interrelated and drawing conclusions on the dependence of each parameter separately on the propagation front movement is very difficult. The other factors that have an influence are related to the bed parameters, like, bed porosity, peak temperature and heat loss from the reactor. It is important to note that the drying, pyrolysis and solid phase combustion of the processes are basically diffusion dominated processes, where the conversion time scales as $t \sim d_o^2$ (d_o is the initial diameter of the particle) [1]. In the case of reduction processes the index ranges between 1 and 1.4 depending upon the reactant, CO_2, H_2O or a mixture, suggesting reaction dependence [1].

1.1. Propagation rate in packed bed

Investigation into the propagation flame front in packed bed gasifiers has been restricted to charcoal, coke and a few studies related to biomass. A number of authors have examined the propagation front rate in the combustion regime against the air stream through a packed bed of solids such as foam, char and wood assuming the combustion front propagation to be one-dimensional [1–15]. The primary emphasis in all these studies has been to predict the flame spread through the porous media. However, very few attempts have been made to study the propagation flame front using different fuels having different physical structure. The process that occurs in a typical wood gasifier is heterogeneous reactions in a packed bed with homogeneous heat release in the gas phase. Pyrolysis releases volatiles leaving behind char. Pyrolysis gases undergo exothermic reactions to yield products which further react with char in endothermic reactions. The reactions that occur in the char bed with several reactants lead to the product gas, containing

* Corresponding author. Tel.: +91 80 23600536.
E-mail address: dasappa@cgpl.iisc.ernet.in (S. Dasappa).

0378-3820/$ – see front matter © 2014 Elsevier B.V. All rights reserved.
http://dx.doi.org/10.1016/j.fuproc.2014.01.011

Table 1
Char combustion and gasification reactions.

Reaction		ΔH (kJ/mol)
Oxidation	$C + O_2 \rightarrow CO_2 + \Delta H$	393.8
Boudouard	$C + CO_2 \leftrightarrow 2CO - \Delta H$	172.6
Water gas	$C + H_2O \leftrightarrow CO + H_2 - \Delta H$	131.4
Water shift	$CO + H_2O \leftrightarrow CO_2 + H_2 + \Delta H$	41.2
Methanation	$C + 2H_2 \leftrightarrow CH_4 + \Delta H$	75

CO, CO_2, CH_4, H_2, H_2O, and N_2. Table 1 presents the char combustion and gasification reactions which occur inside the reactor.

Dasappa and Paul investigated the front propagation rate in a wood-char packed bed reactor (open top down draft gasifier) [1]. This work includes modeling of the reactions of a wood-char sphere with oxygen, steam, and a mixture of CO_2, O_2, and H_2O as a function of particle diameter, ambient temperature, gas composition, and flow velocity. This model has been used to predict the exit gas composition and the propagation rate. The rate processes for the various reactants with char has been evaluated and indicates that the rate of char oxidation with air is higher compared with that for H_2O or CO_2. Ohlemiller et al. formulated a one-dimensional model for smoldering combustion for flexible polyurethane foam assuming thermal equilibrium between gas and solid phases and neglecting the gas phase reactions [2]. This study concludes that the heat transfer process by conduction and convection dictates the smolder propagation rate, and the heat release rate and the smolder velocity are both dependent on the rate of oxygen supply (air supply rate). Dosanjh et al. also developed an analytical model for smoldering front propagation through a porous solid fuel (polyurethane foam and α-cellulose) [3]. Fatehi et al. analyze the downward propagation front in a packed bed of wood particles, where air is supplied from below [4]. In this study, the pyrolysis kinetics is assumed to be much faster than char oxidation for surface heterogeneous reactions. The front speed, the adiabatic temperature and the extent of solid consumption are determined as functions of entering air velocity. The study also examined the oxygen-limited and fuel-limited regimes. In the fuel-limited regime, both the adiabatic temperature and propagation front speed decrease as the air flow rate increases, and as the air flow rate increases an upper extinction limit is reached beyond which the front does not propagate through the medium.

Gort explored the effect of moisture, particle size and volatile components of wood particles, coke and municipal solid wastes in a batch-type grate furnace [5]. It is observed from this study that the propagation rate decreases with the increase in fuel moisture content and the peak propagation rate is shifted towards the lower air mass flux with the increase in moisture content of the fuel. This study shows that the propagation rate has a weak dependence on the size for wood particles, whereas it changes strongly with the size of coke particles. Similar observations were also made by Horttanainen et al. and Rönnbäck et al. [6–8]. Ryan et al. have developed a numerical model for packed bed combustion for char and studied the effect of ash on bed properties and heat and mass transfer during the thermal conversion of fuel [9]. Yang et al. reported that the primary air flow rate has a significant influence on moisture evaporation, devolatilization and char burning [10]. The burning rate increases as the air flow rate increases until a peak point is reached, beyond which a further increase in the air flow rate reduces the burning rate and the burning rate is inversely proportional to the moisture content of the fuel. Porteiro et al. experimentally studied the propagation front in the counter-current process for different biomass fuels and concluded that the air mass flow rate is one of the parameters with the most influence in front propagation velocity [11]. This study reveals that the propagation front does not depend much on the bulk density beyond 400 kg/m^3 [11]. Reed and Markson have done a detailed study on gasification reaction velocities under various conditions in a downdraft gasifier [12]. It concludes that as the biomass pyrolyzed; the gases and vapors mix with the incoming air and form a combustible mixture. Depending on the stoichiometry of the gases, the flame propagates upwards at a relatively higher velocity than the downward velocity of biomass. Hernández et al. studied the effect of particle size and residence time in an entrained flow gasifier using three types of biomass materials [13]. The study concludes that fuel conversion increases (57.5% for 8 mm diameter particles) when reducing the fuel particle size and it leads to an improvement in gasification performance [13]. Yin et al. concluded that as the particle size increases, the gas yield increases while the tar and dust content decreases [14]. Pérez et al. experimental studies concluded that as the equivalent fuel/air ratio decreased, the thermochemical process moved from gasification (fuel rich) to combustion (fuel lean) zone [15].

Table 2 summarizes the results from the literature on various reactor configurations and fuel used. It can be observed from the table that except in the present study, in all other cases, reverse downdraft configurations are used for the experiments and analysis [4,5,7,8,11]. The surface area per unit volume has been calculated for all the cases and it has been found that the surface area per unit volume for wood chips and pine shavings is relatively high compared to that in all other cases. Similarly, the void fraction in the packed bed is also high in these two cases. In all the experiments, except in the present study and Horttanainen et al.'s studies [7], the fuel samples are spherical. The sphericity for all the cases is calculated and it has been found that the sphericity is close to one except in this present study and for wood chips.

In the present study an open top downdraft packed bed system is used simulating the field version where air is drawn for gasification from the top and the nozzle, resulting in the propagation front moving

Table 2
Fuel properties and reactor configurations summary.

Sample	Dimension (mm)	Equivalent radius (mm)	Surface area/volume (mm^{-1})	Sphericity	Density (kg/m^3)		Void fraction	Moisture (%)	Heating value (MJ/kg)	Reactor configuration	Reference
					Bulk	Particle					
Casuarina	14 × 10 × 10	7	0.49	0.889	370	610	0.39	0, 10	18.2	Downdraft	Present study
–	6.4	3.2	0.94	0.998	300	663	0.55	–	14.0	Reverse downdraft	[4][a]
–	10	5	0.60	0.999	200	500	0.60	10	18	Reverse downdraft	[5][b]
Wood chips	5–20	3	1.89	0.561	157	500	0.69	10.8	–	Reverse downdraft	[7][c]
Pine	8	4	0.75	0.999	307	579	0.47	9.1	19.3	Reverse downdraft	[8][d]
Wood pellets	3.8	3.8	0.79	0.999	690	1180	0.42	6.2	16.3	Reverse downdraft	[11][e]
RDF pellets	7.4	7.4	0.41	0.999	340	560	0.39	17.9	14.6	Reverse downdraft	[11]
Pine shavings	1.3	1.3	2.31	0.998	150	530	0.72	8.5	17.5	Reverse downdraft	[11]

[a] Wood particle diameter is 6.4 mm, bulk density is calculated by considering the void fraction to be 0.6.
[b] In this study, 10 mm diameter wood particles are used and the density of the particle is considered to be 500 kg/m^3.
[c] Wood chips are 5–20 mm, the average size 12.5 × 5 × 1.5 mm is considered for surface area per unit volume calculation.
[d] Diameter of the wood particle is 8 mm.
[e] In this study, the fuel particle size is given in equivalent radius.

up from the ignition zone towards the top. This gasification system has air flow shared between the top and the nozzle to stabilize the flame front [16]. The two fold benefits resulting from the distribution of air between the top and the nozzle areas are (a) increasing the char consumption and (b) helping in re-burning of higher molecular weight compounds. These two features provide an excellent means of reducing the tar in the gas and producing consistent gas quality. These benefits have been proved by measurements in the laboratory as well as in the field [16]. While the advantage of sharing of the air between the top and air nozzle is evident, the ratio of air flow rates through the nozzle and the top is critical. Mahapatra and Dasappa reported that an increase in residence time with staged air flow has a better control on residence time of the gas at elevated temperature resulting in lower levels of tar in the raw gas [17]. The propagation rate depends on the ratio of air shared between the top and the air nozzle. Unlike the reported literature, the present co-current configuration needs additional information on the bed shrinkage (size reduction due to volatile release during pyrolysis) or bed movement downward to establish the effective propagation front rate.

This work focuses on the experiments and analysis towards establishing the effect of air mass flux on the propagation rate, bed temperature, gas composition and related aspects under the sub-stoichiometric operating conditions in a downdraft packed bed configuration. It is important to state that the combustion processes occurring in a packed bed are a resultant of both homogenous and heterogeneous reaction process. Depending upon the air flow rate for a given reactor volume and surface area of the bed, the overall process varies between gasification (rich) and combustion (lean) regimes. The present work focuses on establishing an operating regime, where the transformation of energy in the solid fuel is maximized to obtain a mixture of gaseous fuel with maximum chemical energy, i.e., gasification process. Further, in the case downdraft configuration, it is important to consider the propagation flame front along with bed movement to address the overall influence on the temperature profile in the reacting bed. Apart from addressing the packed bed operation in the gasification regime, the effect of mass flow rate which decides the overall air to fuel ratio in the bed which further determines the gas composition and the chemical energy in the gas. Effect of air mass flux in the gasification regime on the propagation rate is also being addressed in this study.

2. Materials and method

The experiments are conducted in a packed bed gasifier as shown in Fig. 1a. The reactor is made up of stainless steel and has 103 mm inner diameter and 1000 mm height. This reactor is insulated with a ceramic blanket throughout its length to reduce the heat losses from it. An air nozzle as shown in Fig. 1a acts as an ignition port. The thermocouple arrangement along the reactor length is also shown in Fig. 1b. The measured parameters during the experiments are gas flow rate, biomass consumption rate, gas composition and bed temperature at different locations along the length of the reactor. The gas flow rate is measured using a calibrated venturimeter, biomass consumption is based on the topping up method, K type thermocouples are used to measure the bed temperatures at various locations of the reactor and an online gas analyser (SICK Maihak: S715 Extractive gas analysers) is used for measuring the different gases like CO, CO_2, CH_4, O_2 and H_2. A high speed data acquisition system (IOtech, PDAQ 56) is used to record the bed temperature. The gas sensors used for measuring different gases in the analyzer are paramagnetic sensor (OXOR-P) to determine the oxygen concentration, infrared sensor (FINOR) which operates with the interference filter-correlation (IFC) principle for measurement of CH_4/CO_2/CO and thermal conductivity sensor (THERMOR) for measurement of H_2 concentration in the gases respectively. The gas composition measurement range for $CO/CO_2/H_2$ is 0–100% and for O_2/CH_4 is 0–25% by volume respectively. The gas analyzer is pre-calibrated using calibrated gas cylinder, in a range of producer gas composition. The sampling flow rate is kept at 1–2 l/min. The gas is cooled by passing through a copper coil dipped into water and later on cleaned by passing the gas through a cotton filter with a layer of calcium chloride for moisture removal. The gas composition data is acquired every 30 s. Output gas and oxygen

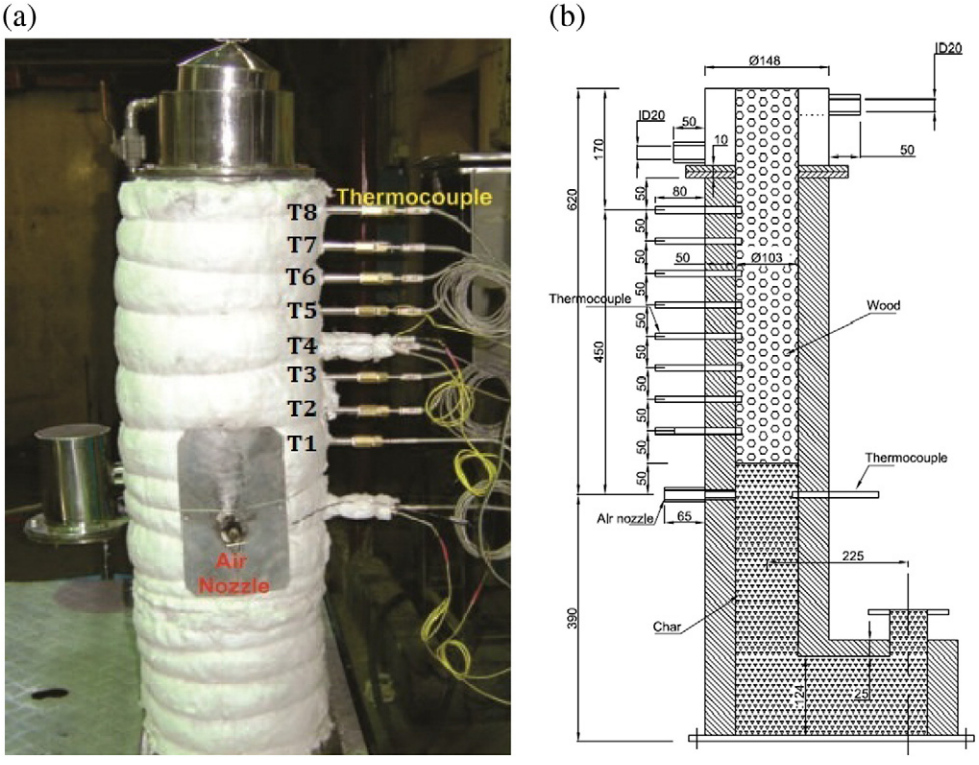

Fig. 1. (a) Air nozzle and thermocouple arrangement in the reactor. (b) Thermocouple arrangement in the reactor.

Table 3
Fuel properties.

Sample	Size (mm)	Moisture (%)	Particle density (kg/m^3)	Bulk density (kg/m^3)
Casuarina	14 × 8 × 8	Sample 1: 0 Sample 2: 10	610	370

Ultimate analysis		Proximate analysis	
Parameter	(% d. b.)	Parameter	(% d. b.)
C	42.83	Fixed carbon	18.38
H	6.236	Volatile matter	81.28
N	0.124	Ash content	0.34
S	0.419	Calorific value (MJ/kg)	18.2

flow rates are measured using pre-calibrated flow meters. Temperature acquisition frequency is 5 s. The acquired data was saved on a computer for further analysis. Experiments are conducted with different gas flow rates (air mass flux) and for different values of moisture content in the biomass. Casuarina (*Casuarina equisetifolia*) wood is used as fuel in the gasifier. The properties of the fuel used in the experiments are presented in Table 3.

Initially the reactor is loaded with charcoal up to the ignition port and for the rest of its height is filled with wood chips of a particular size. A blower is used to provide the required suction to draw the air through the top and the nozzle. After ignition, the air nozzle is closed, allowing all the air to be drawn from the top for the gasification process. During this period, the temperature at various locations and the gas composition are recorded. The bed movement and biomass consumption are measured at specific intervals during the experiments. The output gas is cooled and cleaned before flaring.

The flame propagation rate is calculated by knowing the distance between two consecutive thermocouples and the time required to reach a particular temperature between those thermocouples. The distance between two consecutive thermocouples is 50 mm. The time required to reach the reference temperature between two consecutive thermocouples is calculated by using the temperature profile. The temperature measurement at different locations along the length of the reactor suggests that the temperature profile is well established around 773 K (500 °C) for a range of mass fluxes chosen in the present study. Further, it is evident from Fig. 2 that the time scale between 500 °C and 900 °C is not different, thus choosing 500 °C where there is no change in the temperature profile is justified. Also the slope of all the profiles (at different sections) in this temperature is approximately same. Hence, the reference temperature for calculation of flame propagation is chosen at 773 K (500 °C) in all sets of experiment. The flame propagation rate is calculated by using the following relation

$$\text{Flame propagation rate (mm/s)} = \frac{\text{Distance between the thermocouples (mm)}}{\text{Time required to reach the reference temperature (s)}}.$$

In the counter flow (reverse downdraft) configuration, air comes from below and both the flame front and bed move in the downward direction. However, in the co-current (downdraft) configuration, the bed movement (contributed by size reduction during pyrolysis and fuel consumption) is in the downward direction and the flame front movement into the fuel bed in the upward direction against the air flow. Effective propagation rate is calculated as a sum of flame propagation rate and bed movement. Hence, in case of downdraft configuration, the effective propagation rate has two components, the front velocity (flame propagation rate) moving into the virgin fuel bed against both the air flow and the fuel bed, and the bed movement moving downwards. All these experiments are performed in sub-stoichiometric or gasification regimes only. In the present study, the flame propagation, bed movement and effective propagation rates are obtained for different air mass flux values. Experiments are conducted for obtaining the propagation rates using bone-dry wood particles and wood with 10% moisture.

3. Experimental results

Fig. 2 represents the typical temperature profile inside the reactor over a two-hour period for a air mass flux of 0.12 kg/m^2-s. The propagation front is seen moving from the ignition port towards the top of the reactor in the fuel bed with time. The downstream of the flame front, i.e., below the ignition nozzle, has a slightly lower bed temperature due to the reduction reactions that occur during the process. Fig. 3 presents the flame front propagation, bed movement and the effective front movement variation for bone-dry wood sample in the co-current configuration over a range of air mass flux. The flame propagation front is derived from the axial temperature profile along the length of the reactor. The bed movement is an indication of the biomass consumption due to bed shrinkage factor resulting from pyrolysis and char consumption, shows a nearly linear variation with the air mass flux. The flame propagation rate initially increases, reaches a maximum and then decreases with increasing air mass flux. The peak flame propagation rate is 0.089 mm/s at 0.132 kg/m^2-s air mass flux for bone-dry wood. For the range of air mass flux used in the system, the effective propagation rate reaches a maximum of 0.21 mm/s at 0.147 kg/m^2-s air mass flux and is nearly constant beyond.

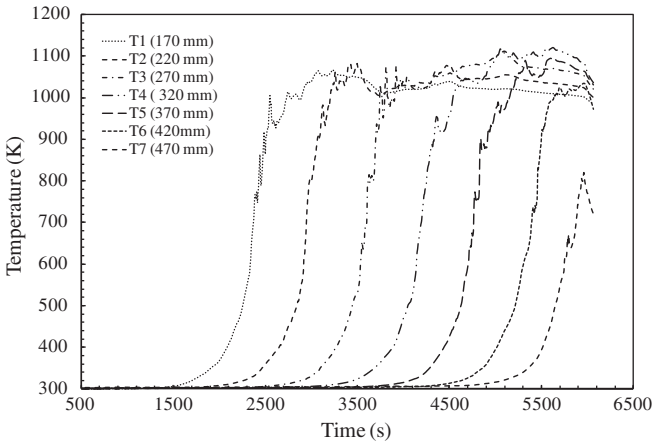

Fig. 2. Temperature profiles inside the reactor at an air mass flux 0.12 kg/m^2 s.

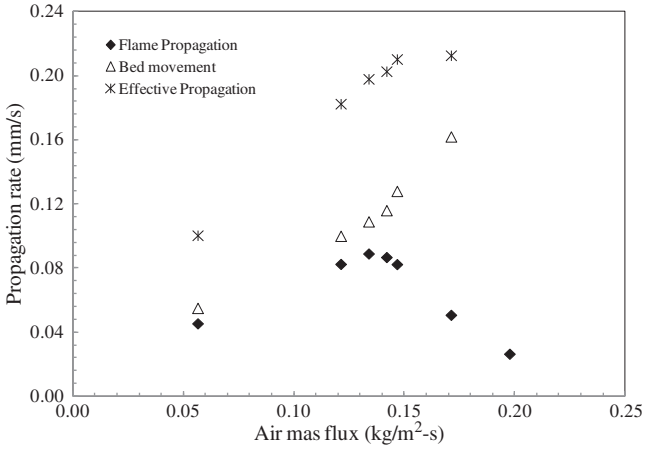

Fig. 3. Propagation rate for bone-dry wood at different air mass flux.

The variation of flame front propagation rate and peak bed temperature with air mass flux for different moisture content is presented in Fig. 4. It is evident from Fig. 4 that the flame propagation rate initially increases as the air mass flux is increased, reaching a peak propagation rate at a certain air mass flux, and further increase in the air mass flux results in a decrease in the flame propagation rate, both for bone-dry wood and 10% moist wood. However, the peak bed temperature increases with the increase in air mass flux. Increasing the air mass flux is accompanied by a higher flame front propagation rate, with increased heat generation in the reaction zone. The peak flame front propagation rates are 0.089 mm/s for 10% moist wood and 0.095 mm/s for bone-dry wood. These peak propagation rates occur with the air mass flux in the range of 0.130 to 0.134 kg/m^2-s. The experiments also revealed that the flame front propagation rate decreases with the increase in moisture content of the fuel. This is due to the endothermicity involved in drying of the moist wood. In the present case the propagation rate for bone-dry wood is about 6% higher than that for wood with 10% moisture content. The trend of flame front propagation in the present case is very similar to that observed by Dasappa and Paul for charcoal in the downdraft configuration [1]. It is also evident from Fig. 4 that the peak bed temperature increases with the increase in air mass flux. Increase in air mass flux increases the heat release in the bed, which corresponds to higher bed peak temperature. However, there is not much variation of peak temperature for bone-dry wood and 10% moist wood and the peak bed temperature is about 1100 K.

Fig. 5 represents the effective propagation rates at various air mass flux values. Presenting the results using effective propagation rates is appropriate to compare the propagation rate from the literature with different experimental configurations (downdraft/co-current or reverse downdraft/counter co-current). The effective front movement increases with the air mass flux rate until a certain mass flux and after that it is found that the rate has a declining trend. The effective propagation rate for the present experiments is compared with those in the experiments of Gort, Horttanainen et al., Rönnbäck et al. and Porterio et al. [5,7,8,11]. It can be observed from Fig. 5 that, except for wood chips (Horttanainen et al.) and pine shavings (Porterio et al.) [7,11], all the other results fall in a narrow band, within experimental error limits considering varying configurations and test conditions. The surface area per unit volume for wood chips and pine shavings are relatively high compared with the other cases. However, the bulk density of these two fuels is very low compared to the other fuels (Table 2). The effect of bulk density on effective propagation will be discussed later.

Fig. 6 presents the average cold gas composition (CO, CO_2, H_2 and CH_4) at the exit of the cooling and cleaning system of the gasifier, along with estimated calorific value at different air mass flux values for both bone-dry and 10% moist wood. The variation of calorific value for bone-dry wood is between 3.4 and 3.8 MJ/kg and for 10% moist wood, it is 3.4 to 4.1 MJ/kg over the entire air mass flux range. The calorific value is lower than the measured value for a field system of larger capacity, which is in the range of 4.5 ± 0.1 MJ/kg [16]. The reason for lower calorific value is probably the scaled down nature of this small capacity reactor, which has higher heat loss per unit surface area of the reactor. However, these considerations are not part of the present investigations. The CO concentration is almost constant throughout the air mass flux range for both bone-dry wood and 10% moist fuel. The hydrogen fraction is slightly different in these cases and the balance is established by CH_4 change in both the cases. Table 4 provides the average gas composition and calorific value over the entire range of air mass flux for bone dry and 10% moist wood. It can be concluded from Table 4 that over the entire range of air mass flux, the gas composition is near constant and it suggests that the overall reaction occurs in the sub-stoichiometric regimes within the bed. It is also found from the equilibrium analysis that to achieve this type of gas composition, the air to fuel ratio is expected to be in the range of 1.5 to 1.8, a typical condition for the gasification process.

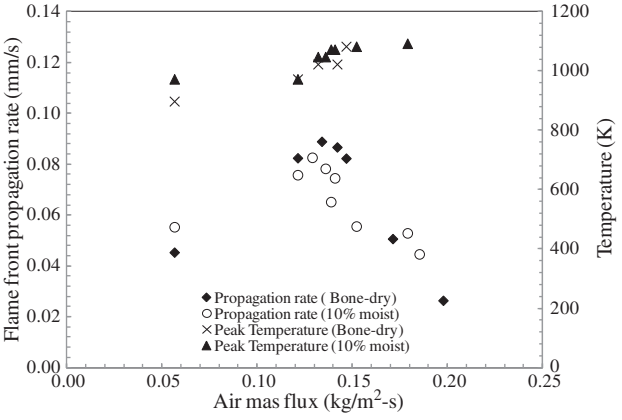

Fig. 4. Flame front propagation rate and peak temperature for different air mass flux.

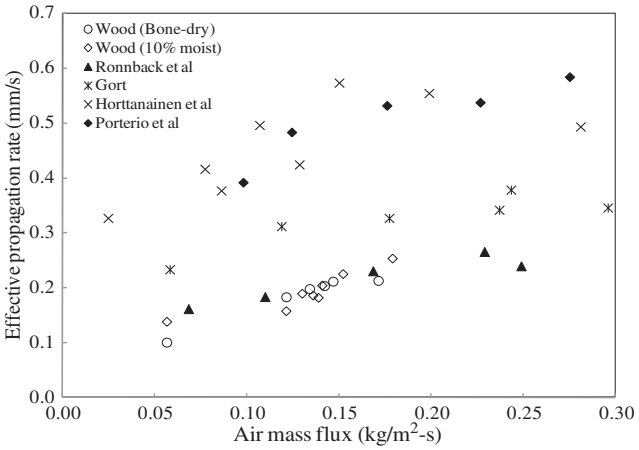

Fig. 5. Effective propagation rate at different air mass flux.

4. Discussion

4.1. Single particle analysis

The entire process of wood combustion consists of distinct flaming and glowing combustion processes. During flaming, volatiles are released and react with the air surrounding the particle resulting in the oxidation of the pyrolysis gases. Glowing combustion is the conversion of char either by reaction with air or with the other reactants like H_2O or CO_2. The flaming and glowing times for wood and briquette spheres for various diameters and presented in Table 5. It can be observed from Table 5 that the flaming time for a 10 mm wooden sphere with a density of 620 kg/m^3 is about 60 s and the glowing time is about 250 s [18]. Whereas for the briquettes of the same diameter with a density of 910 kg/m^3, the flaming time is almost the same, and the char glowing time is 450 s. Hence, it can be concluded that the flaming process is independent of particle density and char glowing process shows a distinct effect of density. This result is similar to the results of Varunkumar et al. [19]. The glowing time is found to be about 4 to 5 times higher in comparison to the flaming time, which suggests that the heterogeneous char reaction is much slower than the flaming process. Hence, it can be inferred from the time scales that flaming pyrolysis dominates during the conversion process. The char conversion occurs after the propagation front moves into the virgin fuel bed. This time for conversion further increases in CO_2 and H_2O environment compared with air. Supporting evidence towards this conclusion is that in the case of counter flow configuration, the top char layer is seen glowing only towards the end of char conversion, which is also reflected in the weight loss,

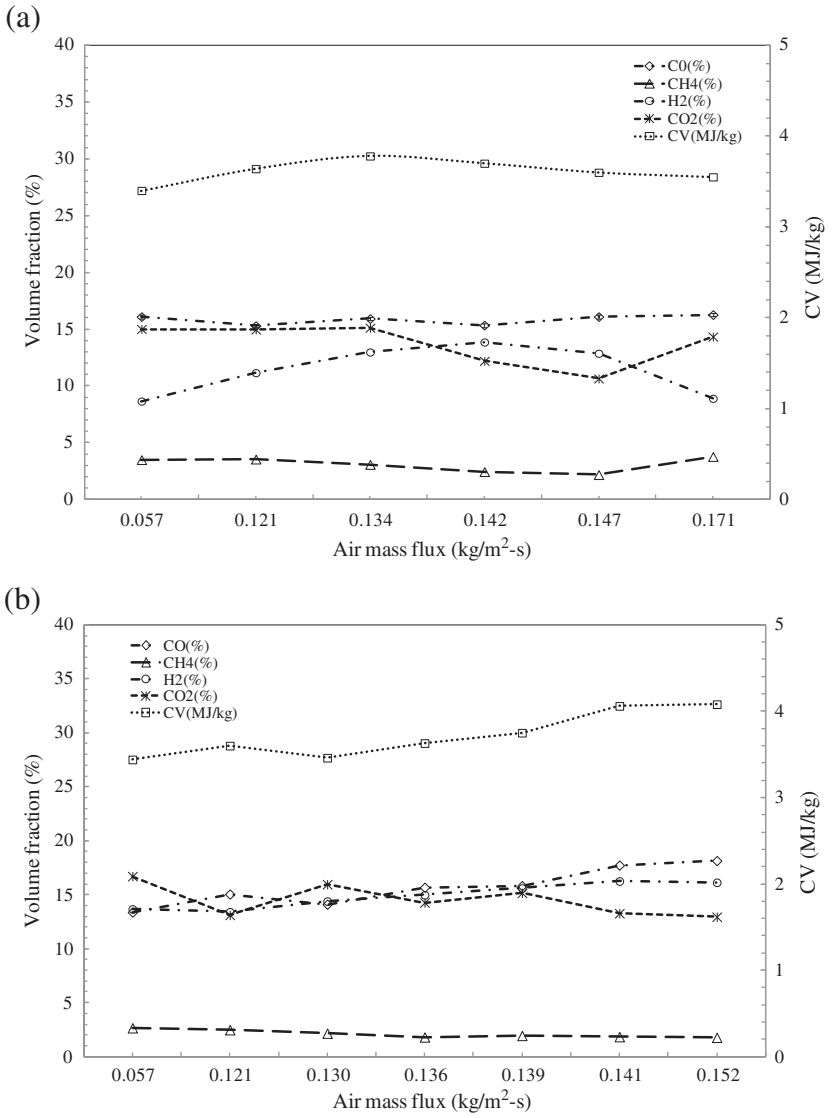

Fig. 6. Gas composition and calorific value at different air mass flux for (a) bone-dry (b) 10% moist wood.

which is significantly lower compared with that in the case of flaming pyrolysis.

Earlier work in this laboratory has shown that the typical particle size shrinkage is about 10–12% during flaming combustion, which affects some of the bed parameters in a packed bed configuration [20,21]. As the devolatilization rate depends on the conditions in the vicinity of the particle, like temperature and composition, with increase in air flow rate, both heat and mass transfer processes influence the pyrolysis rate. Simmons and Ragland have conducted experiments on a single particle at higher flow rate and indicate that both the flaming and glowing processes are affected by a change in the Reynolds number [22]. Thus, the flow past the particles in the packed bed is influenced by the local flow velocity. Hence, it can be concluded that the rate of pyrolysis per unit area of the bed changes with flow, which influences the combustion process of the gaseous species and hence the propagation front. The char oxidation occurs at different time scales. It is found in the various studies that beyond a certain mass flux, the air to fuel ratio for the pyrolysis gases moves away from the stoichiometric condition towards a leaner mixture in the reaction zone, resulting in lower bed temperature [23]. Further, the endothermic reactions also cause reduction in the bed temperature.

Biomass weight loss with time has been measured and mass loss for three different fuels with time plot is shown in Fig. 7. Here also, two distinct modes of combustion can be observed, namely flaming and char mode. It can be observed from Fig. 7 that most of the volatiles are released in the beginning of the process and volatile combustion is manifested as flame propagation similar to that for a premixed gaseous fuel

Table 4
Average gas composition and calorific value for bone-dry and 10% moist wood.

Wood	CO (%)	CO_2 (%)	CH_4 (%)	H_2 (%)	CV (MJ/kg)
Bone-dry	15.83 ± 0.42	13.70 ± 1.86	3.08 ± 0.65	11.40 ± 2.21	3.62 ± 0.13
10% moist	15.70 ± 1.75	14.49 ± 1.49	2.10 ± 0.35	14.92 ± 1.15	3.71 ± 0.26

Table 5
Flaming and char glowing time for wood and briquette spheres [18].

Diameter (mm)	Flaming time (s)		Char glowing time (s)	
	Wood	Briquettes	Wood	Briquettes
10	60 ± 5	55 ± 8	220 ± 8	450 ± 10
15	120 ± 6	134 ± 10	500 ± 10	757 ± 15
20	200 ± 6	160 ± 15	750 ± 13	970 ± 20
25	270 ± 8	265 ± 18	950 ± 15	2154 ± 22

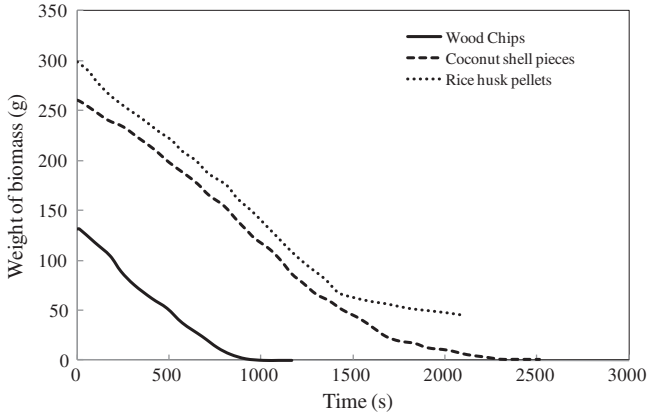

Fig. 7. Biomass weight losses with time.

air mixture. The variation of air mass flux changes the equivalence ratio for the volatile–air mixture. This process can be viewed as a simplified flame speed occurrence in the case of premixed flames. On the basis of these aspects, the packed bed can be viewed as a packed bed of fuel, gas and air mixture with heat loss to the particles and the surfaces. The above aspect has been stated in general terms by Yang et al. by indicating that the consumption of char during the flame propagation in the packed bed is very slow [23]. As the char combustion rate is significantly lower than the devolatilization rate, the char conversion process occupies 1/2 of the total bed length, whereas fuel devolatilization occupies only around 1/3 of the bed length [23]. However, these aspects are subjective and the scientific explanation for such a phenomenon is highlighted in the previous paragraphs.

4.2. Packed bed analysis

In the flame front propagation profile (Fig. 4), a balance is established between heat generation by chemical reactions, radiant heat transfer to the unburnt fuels, convective cooling by primary air, and heat loss rate from the reactor surface. At lower air mass flux, pyrolysis is slower, resulting in lower heat generation as the amount of oxygen is limited. As the oxygen fraction increases, the heat generation increases because the oxidizing environment improves the bed temperature and the flame front propagation rate also increases. When the flame front propagation rate reaches its maximum (peak), the heat generation from the fuel is higher. In the peak flame front situation, a balance is established between the heat generation by chemical reactions and the heat transfer to the unburnt fuels, convective cooling and the heat loss from the reaction zone. As the air mass flux increases from the region of the peak flame front, convective cooling dominates or the net heat loss increases. Various studies provide similar explanations for the variation of propagation rate with air mass flux [5–8,10,11].

4.3. Effect of air mass flux on propagation rate

The present results on the effective propagation rate with respect to air mass flux compare well with the general trends presented in the literature (Gort, Horttanainen et al., Rönnbäck et al. and Porterio et al.) [5,7,8,11]. It can be observed from Fig. 5 that except for wood chips and pine shavings, in all other cases, the experimental results from the literature fall in a narrow band. Higher ignition flux is achieved for wood chips (Horttanainen et al.) and pine shavings (Porterio et al.) as fuel [9,11]. It is important to highlight that for the range of air mass flux (gasification regime) the effective propagation front reaches a peak of about 0.2 mm/s. Beyond a certain air mass flux, propagation rate decreases with an increase of the air mass flux, but the bed movement increases with the air mass flux in the co-current configuration. The attributes to these two factors are different. The reason for increasing propagation with increasing in mass flux is a result of, higher heat transfer coefficient. It also related with higher Reynolds number which in turn is influenced by the air mass flux. Hence, as the air mass flux increases, the propagation rate also increases. However, beyond a certain air mass flux, the heat loss term dominates and reduces the propagation rate. While in case of bed movement, the rate of increase in bed movement (fuel size shrinkage and consumption) is much higher than the rate of decrease in the propagation flame front. This also can be observed from Fig. 5; at lower air mass flux the rate of effective propagation is much higher and at higher mass flux ranges the rate is almost constant.

4.4. Effect of moisture on propagation rate

There is a distinct variation in the propagation rate with moisture variation (Fig. 4). Yang et al. state that the peak flame front propagation rate is inversely proportional to the moisture content of the fuel [23]. However, this is not evident from their data on the inverse dependence. However, it is true that the endothermicity during drying of the fuel affects the propagation rate. Further, it is not evident from the data presented by the authors that higher moisture content in the fuel results in higher moisture evaporation rate and intensifies the char burning, but reduces the devolatilization rate [23]. The possible explanation for this phenomenon is that if the bed temperature is to be maintained; with increase in H_2O content in the reactive environment, the char conversion is higher compared with the case of CO_2 based on the reactivity of char with steam and CO_2. Comparing the conversion time for different reactive environment [1], it has been shown that the conversion time depends on the reactive ambient and the particle size. Horttanainen et al. and Porterio et al. also conclude that higher moisture content in the fuel lowers the maximum ignition flux achieved, regardless of any other parameters [7,11]. The peak flame front rate for bone-dry wood shifts at higher air mass flux compared to that for moist wood as seen in Fig. 4. This aspect is related to the fraction of combustibles generated in the bed. With increase in moisture content both temperature and volatile fraction in the gas phase change and influence the combustion process that occurs within the packed bed. It may be noted that this aspect is similar to an increased heat loss from the reaction zone reducing the peak propagation rate. It is also observed from Fig. 4 that the peak flame temperature rises with the increase of primary air flow rate. At lower air mass flux, the moist fuel has slightly higher peak flame temperature than bone-dry wood. However, for higher air mass flux ranges moisture did not have any noticeable effect on the maximum bed temperature. Similar observations were also made by Horttanainen et al. and Yang et al. [7,23]. These aspects are related to the amount of moisture and volatiles released in the reaction zone and need further investigations.

4.5. Effect of particle surface area on propagation rate

It can be observed from Table 2 that the surface area per unit volume for wood chips and pine shavings is 1.89 and 2.31 (mm^{-1}) respectively and for all the other cases, this value ranges from 0.4 to 0.9 (mm^{-1}). Horttanainen et al. conclude that the increase in bed porosity makes the flame propagation quicker, since the thermal energy needed to heat the bed volume to the ignition temperature is reduced when bed density decreases and the particle surface area to particle volume ratio increases [7]. It is observed from Fig. 5 and the discussion on the packed bed analysis in the previous section, that the higher front movement is observed in the case of wood chips and pine shavings. This is due to the higher surface area per unit volume as a result of smaller particle size and shape. Similarly, the bulk densities of wood chips and pine shavings are much lower than the bulk densities of all other fuels and hence the void fraction is higher compared to other fuels. Lower surface area/volume ratio reduces the inter-particle heat transfer and leads to lower propagation rate. It is also to be noted that the time for pyrolysis

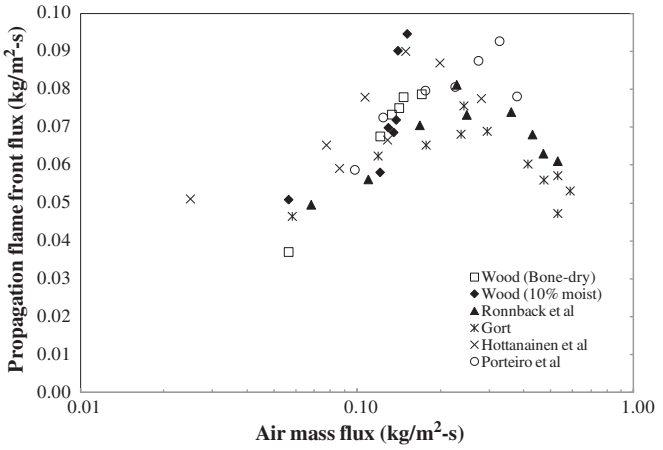

Fig. 8. Propagation flame front fluxes at different air mass flux.

is inversely proportional to the surface area, thus increasing the surface area increases the pyrolysis rate for the same temperature. Further, it is clear that the propagation rate depends on the surface area and bed porosity. The higher the surface area, the higher will be the heat transfer rate process; while an increase in the void fraction tends to reduce the heat transfer coefficient but again radiative heat transfer becomes prominent [1], which compensates for the convective mode of heat transfer. The combination of higher surface area per unit volume and void fraction together enhances the heat transfer from the hot zone to the colder particle layer. Thus, the high surface area per unit volume and the lower bulk density are the reasons for higher propagation rate for wood chips and pine shavings. Hence, the propagation flame front with thin particles is high compared to that for particle beds that consist of spherical or cubical particles. Further, it is also important to mention that the surface area per unit volume is a more important parameter than the size of the particle. Gort and Horttanainen et al. show that the particle size does not have a significant effect on the effective propagation rate [5,7]. The scatter in Fig. 5 can be attributed to the differences in the physical properties of the fuel used in experiments by various authors.

Fig. 8 represents the propagation flame front flux (kg/m^2-s) at different air mass flux values. The flame front flux is defined as the flame front speed normalized with the bulk density. It represents the amount of fuel ignited per unit area per unit time. It can be observed from Fig. 8 that the results for wood chips and pine shavings are nearly the same in comparison with the other data from the literature. Thus, it may be appropriate to normalize the flame propagation rate with the bulk density to account for any variation in the bed properties. Hence, it can be concluded that the front velocity has a direct correlation with the density of the fuel bed. Horttanainen et al. also found similar kinds of results [7]. It is evident that the physical properties of the fuel like particle shape and size, bed density, particle density, energy content of fuel and moisture content influence the effective front movement. However, it is very difficult to specify a single parametric dependence on the front propagation rate.

5. Conclusions

The paper reports results from experimental investigation using a co-current configuration to understand the propagation rate in a packed bed under gasification conditions. It has been shown that the effective propagation rate in a co-current reactor is a combination of flame front movement and bed movement unlike in a counter current reactor. It is found that the flame front rate initially increases as the air mass flux is increased, reaching a peak propagation rate, and further increase in the air mass flux results in a decrease in the propagation rate. The bed movement linearly increases with air mass flux. It is also important to conclude that over the entire range of air mass flux investigation, the calorific value of the output gas is nearly constant.

An attempt has been made to compare various other experimental data from the literature with the results of this study. It has been found that the effective propagation rate compares well and the results are found to lie in a narrow band except for the cases of wood chips and pine shavings. These differences are shown to be due to the high surface area per unit volume and the low bulk density of wood chips and pine shavings. Further, it has been shown that normalized propagation rate or the ignition mass flux is a better way to present the result to account for density variation. However, it can be concluded that the physical properties of the fuel like particle shape and size (surface area per unit volume), bed density, particle density, energy content of fuel and moisture content together have an impact on propagation front movement.

References

[1] S. Dasappa, P.J. Paul, Gasification of char particles in packed beds: analysis and results, International Journal of Energy Research 25 (12) (2001) 1053–1072.
[2] T.J. Ohlemiller, J. Bellan, F. Rogers, A model of smoldering combustion applied to flexible polyurethane foams, Combustion and Flame 36 (1) (1979) 197–215.
[3] S.S. Dosanjh, P.J. Pagni, C.A. Fernandez-Pello, Forced cocurrent smoldering combustion, Combustion and Flame 68 (2) (1987) 131–142.
[4] M. Fatehi, M. Kaviany, Adiabatic reverse combustion in a packed bed, Combustion and Flame 99 (1) (1994) 1–17.
[5] R. Gort, On the propagation of a reaction front in a packed bed, thermal conversion of municipal solid waste and biomass, PhD Thesis University of Twente, 1995.
[6] M. Horttanainen, J. Saastamoinen, P. Sarkomaa, Operational limits of ignition front propagation against airflow in packed beds of different wood fuels, Energy & Fuels 16 (3) (2002) 676–686.
[7] M. Horttanainen, J. Saastamoinen, P. Sarkomaa, Ignition front propagation in packed beds of wood particles, IFRF Combustion Journal (2000)(Article Number 200003).
[8] M. Rönnbäck, M. Axell, L. Gustavsson, H. Thunman, B. Leckner, Combustion processes in a biomass fuel bed — experimental results, Progress in Thermochemical biomass conversion2001. 743–757.
[9] J.S. Ryan, W.L.H. Hallett, Packed bed combustion of char particles: experiments and an ash model, Chemical Engineering Science 57 (18) (2002) 3873–3882.
[10] Y.B. Yang, V.N. Sharifi, J. Swithenbank, Effect of air flow rate and fuel moisture on the burning behaviours of biomass and simulated municipal solid wastes in packed beds, Fuel 83 (11–12) (2004) 1553–1562.
[11] J. Porteiro, D. Patiño, J. Collazo, E. Granada, J. Moran, J.L. Miguez, Experimental analysis of the ignition front propagation of several biomass fuels in a fixed-bed combustor, Fuel 89 (1) (2010) 26–35.
[12] T.B. Reed, M. Markson, Biomass gasification reaction velocities, in: R.P. Overend, T.A. Milne, L.K. Mundge (Eds.), Fundamentals of Thermochemical Biomass Conversion, Elsevier Applied Science Publishers, England, 1982, pp. 951–965.
[13] J.J. Hernández, G. Aranda-Almansa, A. Bula, Gasification of biomass wastes in an entrained flow gasifier: effect of the particle size and the residence time, Fuel Processing Technology 91 (6) (2010) 681–692.
[14] R. Yin, R. Liu, J. Wu, X. Wu, C. Sun, C. Wu, Influence of particle size on performance of a pilot-scale fixed-bed gasification system, Bioresource Technology 119 (2012) 15–21.
[15] J.F. Pérez, A. Melgar, P.N. Benjumea, Effect of operating and design parameters on the gasification/combustion process of waste biomass in fixed bed downdraft reactors: an experimental study, Fuel 96 (2012) 487–496.
[16] S. Dasappa, P.J. Paul, H.S. Mukunda, N.K.S. Rajan, G. Sridhar, H.V. Sridhar, Biomass gasification technology — a route to meet energy needs, Current Science 87 (7) (2004) 908–916.
[17] S. Mahapatra, S. Dasappa, Influence of surface area to volume ratio of fuel particles on gasification process in a fixed bed, Energy for Sustainable Development (2013), http://dx.doi.org/10.1016/j.esd.2013.12.013.
[18] P.M. Gnanendra, D.K. Ramesha, S. Dasappa, Preliminary investigation on the use of biogas sludge for gasification, International Journal of Sustainable Energy. 31 (4) (2012) 252–267.
[19] S. Varunkumar, N.K.S. Rajan, H.S. Mukunda, Single particle and packed bed combustion in modern gasifier stoves-density effects, Combustion Science and Technology 183 (11) (2011) 1147–1163.
[20] H.S. Mukunda, P.J. Paul, U. Shrinivasa, N.K.S. Rajan, Combustion of wooden spheres — experiments and model analysis, Symposium (International) on Combustion (1984) 1619–1628.
[21] S. Dasappa, P.J. Paul, H.S. Mukunda, U. Shrinivasa, Wood-char gasification: experiments and analysis on single particles and packed beds, Symposium (International) on Combustion 1 (1998) 1335–1342.
[22] W.W. Simmons, K.W. Ragland, Burning rate of millimeter sized wood particles in a furnace, Combustion Science and Technology 46 (1) (1986) 1–15.
[23] Y.B. Yang, V.N. Sharifi, J. Swithenbank, Substoichiometric conversion of biomass and solid wastes to energy in packed beds, AIChE Journal 52 (2) (2006) 809–817.